Non-linear Ballooning Mode Theory and Consequences for ELMs in Tokamaks

H. R. Wilson, S. C. Cowley[2], A. Kirk and P. B. Snyder[3]

EURATOM-UKAEA Fusion Association, Culham Science Centre, Abingdon, UK
[2]UCLA, Los Angeles, California 90095 USA
[3]General Atomics, San Diego, California 92186-5608

Email contact of main author: howard.wilson@ukaea.org.uk

Abstract. A theory for the early non-linear evolution of ballooning modes is developed for tokamaks from an ideal magneto-hydrodynamic model of the plasma. The solution procedure depends on the Mercier stability parameter, which, in turn, depends on the shaping of the tokamak plasma: three different regimes are identified. The theory predicts that when the pressure pedestal is close to linear marginal stability, the ballooning mode will grow explosively, driven by non-linear terms, which act to weaken the field line bending. The mode structure evolves to form a number of hot plasma filaments that are ejected into the scrape-off layer on the outboard side, but remain connected into the core plasma on the inboard side. Initial results from large-scale simulations show features that are consistent with such structures. Possible mechanisms for how the filaments could lead to heat and particle loss during the ELM are proposed.

1. Introduction

The size of edge-localised modes, or ELMs, on ITER remains one of the most important issues for the design of the device. These repetitive, explosive events are associated with the edge transport barrier of H-mode plasmas, and can result in large transient heat loads on the target plates. They are a serious concern for ITER because they could possibly prevent operation with the best performance plasmas, which typically have the largest ELMs. Each individual ELM event is thought to involve a complicated interaction between magneto-hydrodynamic (MHD) processes and turbulent transport processes. While there has been good progress in developing a model for the trigger for the ELM based on linear ideal MHD theory [1,2,3], there has been relatively little progress with identifying a quantitative model for the energy loss during an ELM. As a step in this direction, we have developed a theory for the early non-linear evolution of the ballooning mode instability [4,5]. This theory, described in Section 2, predicts that hot filaments of plasma will form, and be ejected from the plasma on the outboard (low field) side, while remaining connected into the hot core plasma on the inboard side. The two-fluid MHD code, BOUT [6], has also been used to predict the non-linear nature of instabilities associated with the plasma edge region [7]. There are similarities with the theory presented here, which we demonstrate in Section 3. In order to understand the loss of heat and particles during an ELM, it is necessary to go beyond ideal MHD. We close in Section 4 with a discussion of possible models to be developed further which could in principle lead to heat and particle transport, providing the final ingredient for a complete, predictive model for the ELM cycle.

2. Non-linear ballooning mode theory

The details of the calculation have been presented previously [4,5], so here we limit ourselves to a brief description of the important elements of the theory. We then discuss the method of solution of the resulting non-linear equation describing the evolution of the mode structure in the two directions perpendicular to the magnetic field lines.

Our starting point is the full, non-linear, ideal MHD force-balance equation in Lagrangian coordinates. We write the Lagrangian displacement, $\boldsymbol{\xi}$, in terms of three components:

$$\boldsymbol{\xi} = \xi_\psi \boldsymbol{e}_\perp + \xi_\alpha \boldsymbol{e}_\wedge + \xi_\parallel \boldsymbol{B}_0 \tag{1}$$

where $\boldsymbol{e}_\perp = \nabla\alpha \times \boldsymbol{b}$, $\boldsymbol{e}_\wedge = \boldsymbol{b} \times \nabla\psi$, $\boldsymbol{B}_0 = \nabla\psi \times \nabla\alpha$, $\boldsymbol{B}_0$ is the equilibrium magnetic field, ψ is the poloidal flux and α is a helical angle which labels particular magnetic field lines on a given flux surface. The vector $\boldsymbol{b} = \boldsymbol{B}_0/B_0$ is a unit vector in the magnetic field direction. We work with the variables ψ, α, and θ, where θ is a poloidal angle, measuring the distance along a field line (taken to be effectively infinitely long).

In order to simplify the non-linear equations, we employ a small parameter, ε, which characterises the mode structure. We anticipate an ordering guided by the results of linear ballooning theory, which is likely to be appropriate provided we are sufficiently close to the linear regime:

$$\left.\frac{\partial}{\partial\theta}\right|_{\alpha,\psi} \sim \varepsilon^0, \quad \left.\frac{\partial}{\partial\psi}\right|_{\alpha,\theta} \sim \varepsilon^{-1}, \quad \left.\frac{\partial}{\partial\alpha}\right|_{\psi,\theta} \sim \varepsilon^{-2} \tag{2}$$

Anticipating leading order cancellations in $\nabla\cdot\boldsymbol{\xi}$, we order $\xi_\parallel \sim \xi_\psi$ and $\xi_\alpha \sim \varepsilon\xi_\psi$, with an absolute ordering $\xi_\psi \sim \varepsilon^2$ to avoid shocks. Finally, in order to introduce time dependence in the highest order equations, we assume $\partial/\partial t \sim \varepsilon^{2/\lambda}$, where $\lambda = \lambda_S - \lambda_L$ is the difference between the two Mercier indices [$\lambda_{S,L} = 1/2 \pm (1/4 - D_M)^{1/2}$, with D_M the Mercier coefficient].

As we develop the expansion in ε, we find that the perturbation is incompressible to the first three orders. From the second order force balance equation, we deduce that ξ_ψ satisfies the standard, linear ballooning equation. Neglecting inertia, the solution can then be written in the form

$$\xi_\psi^{(2)} = \hat{\xi}(\psi, \alpha, t) H(\theta; \mu) \tag{3}$$

where $H(\theta)$ is the solution to the marginally stable ballooning equation (the superfix denotes the order in ε). The parameter μ is introduced as a scaling factor on the curvature drive term in the ballooning equation and serves as an eigenvalue (which will be close to unity, provided the equilibrium is close to marginal stability). The small corrections $\sim(\mu - 1)$ will be re-introduced in the higher order equations. Note that $(\mu - 1)$ provides a measure of how close the equilibrium is to marginal stability. Both H and μ have a slow variation with ψ (ie on the equilibrium length scale $\sim\varepsilon^0$).

Before proceeding, let us digress to consider the implications of Eq (3). The condition that inertia can be dropped requires $\theta\partial/\partial t \ll 1$. Thus, sufficiently far along the field line, where $\theta\partial/\partial t \sim 1$, inertia has an $O(1)$ contribution and cannot be treated perturbatively. The solution Eq (3), which neglects inertia, is therefore not valid in this region, and it will be necessary to develop a new procedure in the region far along the field line. This is the first important point.

A second important point can be illustrated by considering the behaviour of H far along the field line, such that $\theta \gg 1$, but $\theta\partial/\partial t \ll 1$ so inertia is not important. In this region, we deduce $|\boldsymbol{e}_\perp|\xi_\psi \sim \theta^{1-\lambda_s}$. Thus, provided the shaping is sufficiently strong that $\lambda_s > 1$, the amplitude of the perturbation decays with distance along the field line. Non-linearities are therefore not important in the region $\theta\partial/\partial t > 1$, which we shall refer to as the "inertial" region. Thus, for $\lambda > 1$ the problem can be split into two separate calculations: (1) to evaluate the perturbation in the "ideal" region, where inertia can be treated perturbatively but non-linearities are important, and (2) to evaluate the solution in the "inertial" region, where non-linearities can be neglected. The solution is completed by matching the results of these calculations in the "matching region" $\theta \gg 1$, $\theta\partial/\partial t \ll 1$ (see Fig 1).

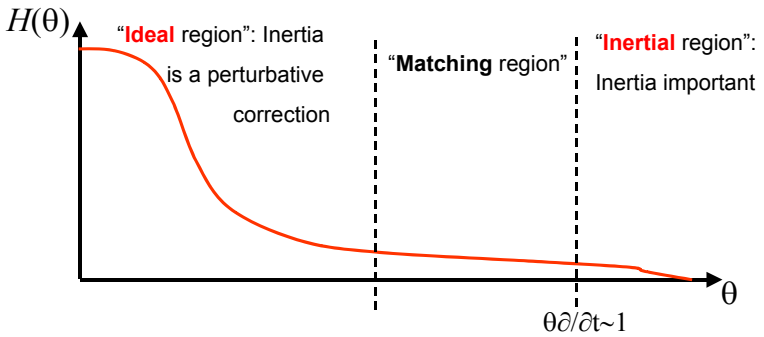

FIG. 1. *Sketch of a typical solution to the ballooning equation showing the "ideal" and "inertial" regions*

Let us now consider this matching procedure. In general, if one is not precisely at marginal stability, the solution in the matching region is a linear combination of the large and small Mercier solutions:

$$\lim_{\theta\to\infty}\xi = a\left(\frac{1}{\theta^{\lambda_L}}+\frac{\Delta'}{\theta^{\lambda_S}}\right) \tag{4}$$

where a and Δ' represent the two constants of integration arising from the solution of the ballooning equation (a 2nd order ODE). In the "ideal" region the boundary condition that determines Δ' is that it must have the same value for both positive and negative θ. Thus, Δ' can be calculated from the "ideal" region alone, and embodies all the non-linearities (when $\lambda_S>1$) . An analagous quantity is identified in the "inertial" region, and depends on the inertia (for more complete plasma models, it could also describe the effects of resistivity, diamagnetic effects, etc). Matching the two results for Δ' provides the complete evolution equation. There is one final subtlety. In the linear theory, the inertial region provides a contribution to the inertia $\sim\gamma^{\lambda}$, while the contribution from the "ideal" region would be $\sim\gamma^2$, where γ is the linear growth rate. Thus, if $\lambda>2$ (ie $D_M<-3/4$) the dominant contribution to the inertia actually comes from the ideal region, and the inertial region plays no essential role. In this case, it is sufficient to neglect the inertial region and apply a "line-tied" boundary condition far along the field line. The theory is then exactly as described by Hurricane et al [8]. However, if $1<\lambda<2$, the inertial region does provide the dominant contribution to the inertia, and its effect cannot be neglected. Here, we develop the theory for this regime, which is often the most relevant at the plasma edge.

To summarise, we have identified three regions of parameter space. (1) For $\lambda>2$ the "ideal" region contains the dominant non-linearities and the dominant contribution to the inertia. The "inertial" region far along the field line can be neglected, and the theory developed in [8] is appropriate. (2) For $1<\lambda<2$, the "ideal" region contains the dominant non-linearieties, but the dominant contribution for the inertia comes from the "inertial" region. This is the theory presented here. (3) For $\lambda<1$, relevant only in the tokamak plasma core, both the non-linearities and the inertia are dominant in the "inertial" region. We leave this region for future work.

Let us now return to derive the solution in the "ideal" region. It is necessary to develop the expansion to two higher orders in ε to evaluate $\hat{\xi}(\psi, \alpha, t)$ (see Eq (3)). These provide a non-linear equation for $\xi_\psi^{(4)}$. After much algebra, one can show that the large θ limit of the solution simply adds a component of the "large" solution (ie $\sim\theta^{-\lambda_L}$) to the "small" solution (ie $\sim\theta^{-\lambda_S}$) contained in $\xi_\psi^{(2)}$ (through H). By integrating out to large θ, across the full ideal region, and identifying Δ' as the ratio of coefficients of small to large solutions (see Eq (4)), we derive the following expression from the ideal region:

$$\lambda \frac{1}{\Delta'} \frac{\partial^2 u}{\partial \alpha^2} = C_1 \left[2(1-\mu) \frac{\partial^2 u}{\partial \alpha^2} - \frac{\partial^2 \mu}{\partial \theta_0^2} \frac{\partial^2 u}{\partial \psi^2} \right] + C_2 \frac{\partial}{\partial \alpha} \left[\left(\frac{\partial u}{\partial \alpha} \right)^2 \right] + C_4 \frac{\partial^2 u}{\partial \alpha^2} \frac{\partial^2}{\partial \psi^2} \overline{\left(\frac{\partial u}{\partial \alpha} \right)^2} \quad (5)$$

where we have written $\partial u/\partial\alpha \equiv \xi$ and the over-bar denotes an integral over α. The parameter θ_0 is the parameter familiar from linear ballooning theory, and is chosen so as to minimise μ. The coefficients C_j represent integrals over θ across the ideal region of functions involving equilibrium quantities and the solution to the linear ballooning equation, H. For $\lambda>1$, the contribution of the inertial region to these integrals is negligible, and then they can be integrated over the full range $-\infty<\theta<\infty$.

Turning now to the inertial region, the linearised equations are conveniently solved by employing a Laplace transform in time. The procedure then follows the standard linear analysis, with the Laplace variable, p, taking the place of the linear growth rate γ. This allows Δ' to be identified. Following analytic inversion of the Laplace transform, the solution for Δ' from the inertial region is:

$$\frac{1}{\Delta'} \frac{\partial \hat{\xi}(\alpha, \psi, t)}{\partial \alpha} = C_0 \frac{\partial^2}{\partial t^2} \frac{\partial}{\partial \alpha} \left[\int_0^t dt' \frac{\hat{\xi}(\alpha, \psi, t')}{(t-t')^{\lambda-1}} \right] \quad (6)$$

Matching the two expressions for Δ' then provides our final evolution equation:

$$\frac{\partial^2}{\partial t^2} \frac{\partial^2}{\partial \alpha^2} \left[\int_0^t dt' \frac{u(\alpha, \psi, t')}{(t-t')^{\lambda-1}} \right] = \left[2(1-\mu) \frac{\partial^2 u}{\partial \alpha^2} - \frac{\partial^2 \mu}{\partial \theta_0^2} \frac{\partial^2 u}{\partial \psi^2} \right] + \frac{\partial}{\partial \alpha} \left[\left(\frac{\partial u}{\partial \alpha} \right)^2 \right] + \frac{\partial^2 u}{\partial \alpha^2} \frac{\partial^2}{\partial \psi^2} \overline{\left(\frac{\partial u}{\partial \alpha} \right)^2} \quad (7)$$

We have absorbed the coefficients C_j into a re-definition of the variables. Let us consider each term in turn. The first square-bracketed term on the right hand side is the contribution from the standard linear drive, composed of a piece reflecting the linear drive, and a piece reflecting the finite toroidal mode number stabilising term. The second term provides an additional non-linear drive. The third term is a cubic non-linearity, which is negative (stabilising) in the region of ψ where u is a maximum, and positive elsewhere. Thus, the effect of this term is to stabilise the linearly unstable region (ie that where $\mu(\psi)<1$) and destabilise flux surfaces in the linearly stable region. Thus, this term has the effect of "spreading" the region affected by the instability in the radial direction. The term on the left is interesting. It is a formal representation of the fractional derivative $\partial^\lambda/\partial t^\lambda$. Recall that we argued earlier that the theory of Hurricane et al [8] is relevant when $\lambda>2$. In this case one obtains precisely Eq (7) (but with different coefficients), except that the term on the left hand side is simply $\partial^2 u/\partial t^2$. Thus our result matches smoothly onto the Hurricane result as λ passes through 2.

Before we consider numerical solutions to Eq (7), we can deduce certain properties of the solution analytically. To derive how non-linearities affect the drive, we suppose we are in the regime where the non-linear terms dominate the linear ones, and balance the inertia against the quadratic non-linearity. This provides the result that

$$\hat{\xi} \sim \frac{1}{(t_0(\alpha, \psi) - t)^r} \quad (8)$$

where $r=\lambda$ for $1<\lambda<2$, and $r=2$ for $\lambda>2$ (the Hurricane result [8]). Note that there is a finite-time singularity at the time $t=t_0$, where t_0 depends on the initial conditions. As one approaches this time, the mode grows explosively, even when the equilibrium profiles are maintained close to the linear marginally stable values (ie where the linear growth rate would be small). Note also that the mode amplitude grows fastest close to where t_0 is a minimum, and therefore this would suggest there is a narrowing of the structure about this position. However, this is not the full picture. To understand the mode structure perpendicular to the field lines in more

detail, let us balance the two non-linear terms. This provides a relationship between the widths in the two directions perpendicular to the magnetic field line:

$$\frac{(\Delta\psi)^2}{\Delta\alpha} \sim \frac{1}{(t_0 - t)^r} \tag{9}$$

Thus, while there is a tendency for the mode to narrow in the α direction, it tends to spread more in the radial direction into the region which is linearly stable.

Let us now turn to the numerical solution of Eq (7). We first reduce this equation to the following system:

$$\frac{\partial h}{\partial t} = F(\xi; \alpha, \psi, t) \qquad \frac{\partial y}{\partial t} = h \tag{10}$$

$$y(\alpha, \psi, t) = \frac{1}{\Gamma(2-\lambda)} \int_{-\infty}^{t} dt'(t-t')^{1-\lambda} \xi(\alpha, \psi, t') \tag{11}$$

We solve these by first specifying "initial" conditions at t=0. The condition we impose is that the solution for ξ at all times t<0 is the linear eigenmode, which has been growing exponentially with the linear growth rate. In addition, the amplitude of ξ is taken to be sufficiently small at t=0 that the non-linear terms are negligible compared to the linear ones. From Eqs (10) and (11) we can then evaluate solutions for $y(t=0)$ and $h(t=0)$.

Knowing y and h at any time $t=t_i$, and ξ for all times $t \le t_i$, we advance the system to $t=t_{i+1}$ as follows. First, we advance h and y from Eq (10) using a standard explicit scheme. Knowing these allows us to the advance ξ by inverting the integral in Eq (11). Because the integrand is divergent at $t'=t_{i+1}$ (though the integral is not), care has to be taken to preserve accuracy in the solution. Thus, we separate the integral into an integral up to t_i and an integral from t_i up to t_{i+1}. We derive an accurate approximation for the integral from t_i to t_{i+1} by Taylor expanding ξ about $t=(t_{i+1}+t_i)/2$, and then performing the integral analytically. After some straightforward algebra, we arrive at the result:

$$\xi_{i+1} = -(2-\lambda)\xi_i + \frac{(2-\lambda)(3-\lambda)\Gamma}{(\Delta t)^{2-\lambda}} \left\{ y_{i+1} - y_i + \frac{1}{\Gamma} \int_{-\infty}^{t_i} \xi(t') \left[\frac{1}{(t_i - t')^{\lambda-1}} - \frac{1}{(t_{i+1} - t')^{\lambda-1}} \right] dt' \right\} \tag{12}$$

where $\Gamma \equiv \Gamma(2\text{-}\lambda)$ is a Gamma function. An interesting feature of this result is the appearance of a fractional power of the time step, $\Delta t = t_{i+1} - t_i$, reflecting the fact that this expression is derived from a fractional derivative. Note, there remains an integral to be performed numerically over all previous times. We have chosen to express the solution in this way, adding and subtracting contributions from y_i, so that there is a leading order cancellation between the two terms in square brackets for times $t' \ll t_{i+1}$ and then the integrand becomes negligible. This improves the efficiency of the numerical scheme somewhat as it reduces the effective range that the integral has to be performed over (note that this integral needs to be computed at each spatial mesh point). The integral is evaluated between successive time mesh points by Taylor expanding $\xi(t')$ about the mid-point of the two mesh points, and performing the remaining integral between the mesh points analytically. This procedure is much more accurate than simply Taylor expanding the whole integrand, particularly as one approaches $t'=t$.

We have evaluated the solution of Eq (7) for λ=1.6 using the above procedure. The instantaneous growth rate, defined by $\gamma(t) = (1/\xi)\, \partial\xi/\partial t$, is shown as a function of time by the full curve in Fig 2. Note that during the initial linear phase, the growth rate is approximately independent of time. As the finite-time singularity is approached, the growth rate increases rapidly, with ξ growing as $(t_0 - t)^{-1.7}$, where t_0=10.5. This is broadly consistent with the analytic prediction of Eq (8). Also shown in the figure is how the width of the mode in the α direction, $\Delta\alpha$, narrows as the time singularity is approached.

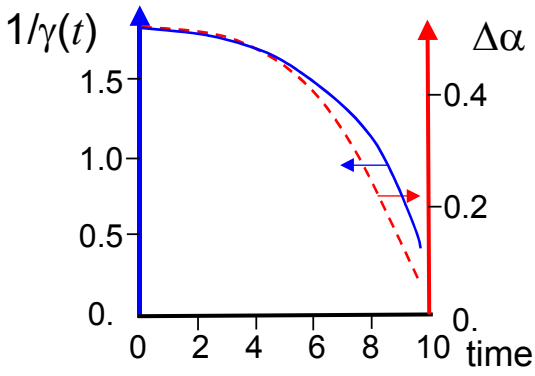

FIG. 2. The instantaneous growth rate, γ(t) (full curve), and the width of the perturbation in the α direction (dashed curve) as a function of time.

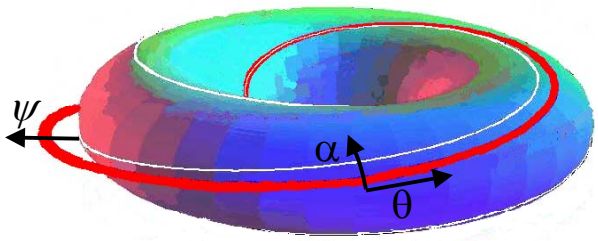

FIG. 3. The red line provides an artist's impression of the filamentary structure into which the ballooning mode evolves. It originated from the white field line. Note, the filament remains close to the field line on the inboard side, but moves far from it on the outboard side.

To summarise, we have found that during the non-linear evolution of the ballooning mode, the plasma develops filamentary structures that are elongated along the field line, but highly localised in the directions perpendicular to the field line. On the outboard (low magnetic field) side of the tokamak plasma, the filaments are displaced radially a large distance from the field line on which they originated. On the inboard side, the radial displacement is much less. A cartoon illustrating this structure is shown in Fig 3.

3. Two-fluid simulations

The 3D BOUT code [6] has been used to explore the pedestal properties in plasmas that are unstable to ballooning modes in the edge region [7]. BOUT is based on a reduced set of Braginskii equations, which are solved in both the pedestal and scrape-off layer regions. A tokamak equilibrium that is linearly unstable to a peeling-ballooning mode is used as the starting point for the calculation. At early times, an n=20 fast-growing linear mode is established, as expected. However, at a later time, there is a sudden burst of activity with an accompanying rapid loss of heat and particles. Figure 3 shows the mode structure in the plane of toroidal angle (one fifth of the toroidal region is shown) versus radius, with the separatrix marked by the vertical dashed line. Figure 3a shows the structure during the linear phase, and is consistent with what is expected from the linear analysis. At a later time, Fig 3b shows the growth of a structure, which is localised in the toroidal direction but shows some tendency to spread in the radial direction. Furthermore, the non-linear structure observed in the BOUT simulations is very extended along a field line [7]. This spatial evolution is consistent with the filamentary structures expected from the non-linear ballooning mode analysis (see Eq (9)). Future work will aim to make more quantitative comparisons between the BOUT results and the non-linear ballooning mode theory, exploring both the spatial structure and the temporal evolution.

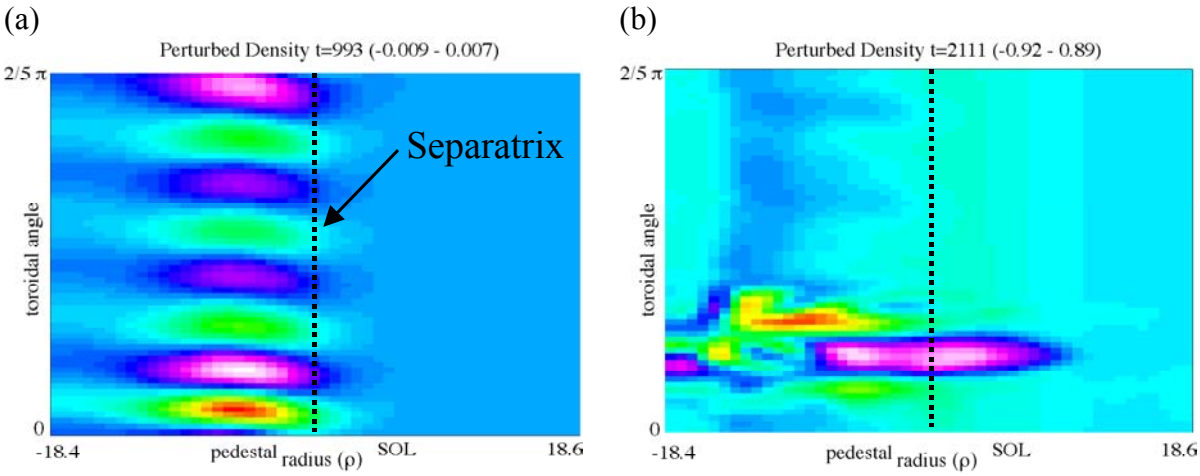

FIG. 3. *Non-linear calculations of edge MHD structures using the BOUT code in the linear phase (a) and a highly non-linear phase (b), during which a filamentary structure is formed.*

4. Discussion

Analytic theory and numerical calculations both indicate that MHD ballooning modes evolve into non-linear structures that result in a filamentation of the plasma. It is now widely believed that ballooning modes, driven unstable by the steep pressure gradient in the edge pedestal region, do play an important role in the dynamics of large (Type I) ELMs in tokamaks. It is therefore natural to ask what role such filamentary structures might have in the rapid loss of heat and particles that occurs during an ELM. There is clear experimental evidence that such filamentary structures do exist during ELM events [9]. However, their role in the loss of heat and particles during the ELM remains unclear. The theory presented in Section 2 is based purely on ideal MHD and therefore cannot lead to any transport. In order to address the transport processes during an ELM, it is necessary to go beyond ideal MHD theory. The rest of this paper provides some speculative remarks on possible mechanisms.

The basic model we propose for the ELM event is the following. At some time, the edge pressure gradient and/or current density drive an ideal MHD mode unstable in the pedestal region. As the mode grows it evolves to form the filamentary structures, elongated along a magnetic field line, but localised about it. On the outboard side, the filament pushes out into the scrape-off layer, but remains connected back into the pedestal region on the inboard side.

When considering how the filaments could, in principle, lead to enhanced heat and particle transport, it is important to realise that the filaments themselves do not carry sufficient energy at any one time to explain the amount of energy loss in an ELM event. Thus, the energy loss cannot be explained simply as a result of the filaments breaking off from the core plasma and depositing their energy in the scrape-off layer. Instead, we propose two possible alternative mechanisms that could be operative.

In the first mechanism it is proposed that the filaments act as conduits, along which heat and particles can flow freely (as this involves transport parallel to the magnetic field lines). Because the filaments connect back into the hot core (pedestal) plasma far along the field lines, they effectively have an infinite reservoir of heat and particles to tap into. It is proposed that the filaments enter the scrape-off layer on the outboard side, so that they provide a direct route for pedestal plasma to reach the scrape-off layer. Of course, within an ideal MHD model, the heat and particles could not leave the filament to enter the scrape-off layer, and additional physics must be invoked to explain this process. One possibility is that the narrowing of the filament leads to sharp pressure gradients, which in turn would enhance diffusive losses from the hot filament into the cooler scrape-off layer. A second possibility is

that these strong pressure gradients could trigger secondary instabilities, which again would enhance the losses from the filament into the scrape-off layer. A particular concern for ITER is that if a filament were to strike the vessel wall, it would impart very large, localised heat loads, which could be very damaging.

A second mechanism is also possible. A filament erupts from the plasma by twisting to squeeze between field lines on adjacent flux surfaces without reconnection (the twisting motion is necessary because of the magnetic shear). However, if there is a strong sheared flow, this process could not occur (our calculations neglected any plasma flow). Either the shear flow would suppress the ballooning mode, or the ballooning mode would suppress the shear flow. We know that there is a strong sheared flow associated with the improved transport in the pedestal region, but the origin of the torques which give rise to this remain uncertain. However, if the $\boldsymbol{J}\times\boldsymbol{B}$ torque associated with the ballooning mode can dominate the driving torque, presumably associated with the L-H transition physics, and bring the pedestal plasma to rest, this would allow the filaments to grow. If that is the case, once the shear flow is suppressed, the plasma would presumably revert to an L-mode state, and the pedestal would collapse. Indeed, as the pressure gradient in the H-mode pedestal could be far above any critical gradient required for turbulent transport in the absence of sheared flow, the resulting heat and particle loss during the ELM could be far higher than even that expected from L-mode discharges. Thus, in this scenario, the filaments would act as a trigger to revert the plasma edge back to an L-mode, rather than be a direct cause of the enhanced transport themselves. Once the pressure gradient in the edge region has collapsed, the ballooning mode would be re-stabilised, allowing the flow shear and pedestal to re-establish, and the process would repeat.

There is clearly much to be done to place this model for the ELM crash on a firmer theoretical basis. Edge turbulence codes will be invaluable here to help clarify the dominant mechanisms. However, the explosive nature of the instabilities, together with a tendency for the MHD structures to evolve to very fine spatial scales, also provide a role for analytical theory to develop qualitative solutions, and to guide the procedures and numerical schemes used to simulate ELMs in the large-scale computer calculations.

References

[1] CONNOR J.W., et al Phys. Plasmas **5** 2687 (1998)
[2] WILSON H.R., et al, Phys Plasmas **6** 1925 (1999)
[3] SNYDER P.B., et al, Phys Plasmas **9** 2037 (2002)
[4] COWLEY S.C., et al, Plas Phys Cont Fus **45** A31 (2003)
[5] WILSON H.R. and COWLEY S.C., Phys Rev Lett **92** 175006 (2004)
[6] Xu X.Q., et al, New J. Physics **4** 53 (2002)
[7] SNYDER P.B., et al EPS Conference Proceedings, London (2004), paper P2.156
[8] HURRICANE O.A., FONG B.H. and COWLEY S.C., Phys Plasmas **4** (1997) 3565
[9] KIRK A., et al, Phys Rev Lett. **92** (2004) 245002-1

Acknowledgements. We thank Jack Connor for many helpful discussions during the course of this work, which was jointly supported by the United Kingdom Engineering and Physical Sciences Research Council and EURATOM.